PERFORMANCE ANALYSIS OF DoA ESTIMATION METHODS FOR SYSTEMS USING LOW-RESOLUTION ADCS

PHÂN TÍCH HIỆU SUẤT CỦA CÁC PHƯƠNG PHÁP ƯỚC LƯỢNG DoA CHO CÁC HỆ THỐNG SỬ DỤNG ADC PHÂN GIẢI THẤP

Vien Nguyen-Duy-Nhat[1]*, Hung Nguyen-Le[2]

[1]*The University of Danang - University of Science and Technology, Vietnam*
[2]*The University of Danang - University of Technology and Education, Vietnam*

*Corresponding author: ndnvien@dut.udn.vn

(Received: April 28, 2025; Revised: June 11, 2025; Accepted: August 05, 2025)

DOI: 10.31130/ud-jst.2025.23(9A).238

Abstract - Direction of Arrival (DoA) estimation is a fundamental task in array signal processing, essential for applications such as radar, sonar, and wireless communications. To reduce hardware complexity, cost, and power consumption, low-resolution analog-to-digital converters (ADCs) have been widely adopted, especially in multi-antenna systems. This paper focuses on analyzing DoA estimation techniques designed for systems employing low-resolution ADCs. It derives the Cramér-Rao Lower Bound (CRLB) to assess the theoretical performance limits of these methods. Through simulations, the study demonstrates that using ADCs with 2 to 3 bits of quantization achieves an excellent balance between performance and hardware efficiency, making them a practical solution for many modern systems. These findings offer valuable insights for the design of energy-efficient and cost-effective communication and sensing platforms.

Key words - DoA; low-resolution ADC; MUSIC; SPICE; Bartlett; CRLB

Tóm tắt - Ước lượng hướng đến (Direction of Arrival – DoA) là một nhiệm vụ cốt lõi trong xử lý tín hiệu mảng, đóng vai trò thiết yếu trong các ứng dụng như radar, sonar và truyền thông không dây. Để giảm độ phức tạp phần cứng, chi phí và tiêu thụ điện năng, các bộ chuyển đổi tương tự–số (ADC) có độ phân giải thấp đã được ứng dụng rộng rãi, đặc biệt trong các hệ thống đa ăng-ten. Bài báo này tập trung phân tích các kỹ thuật ước lượng DoA dành cho các hệ thống sử dụng ADC độ phân giải thấp. Đồng thời, nó cũng xây dựng biểu thức giới hạn dưới Cramér–Rao (CRLB) nhằm đánh giá giới hạn hiệu suất lý thuyết của các phương pháp này. Kết quả mô phỏng cho thấy rằng việc sử dụng ADC với 2 đến 3 bit lượng tử hóa mang lại sự cân bằng tối ưu giữa hiệu suất và hiệu quả phần cứng, trở thành lựa chọn thực tiễn cho nhiều hệ thống hiện đại. Kết quả này cung cấp gợi ý trong thiết kế các nền tảng tiết kiệm năng lượng và chi phí.

Từ khóa - DoA; low-resolution ADC; MUSIC; SPICE; Bartlett; CRLB

1. Introduction

Direction of Arrival (DoA) estimation techniques play a pivotal role in array signal processing, with critical applications spanning fields such as radar, sonar, and wireless communications [1, 2]. Traditional DoA estimation methods typically assume high-resolution digitized signals obtained from ADCs with many quantization bits. However, the manufacturing cost and power consumption associated with analog-to-digital converters (ADCs) increase significantly as the quantization bits and sampling rate rise. When deployed in systems requiring multiple ADCs, such as multi-antenna receivers, both cost and energy consumption become severe issues [3, 4].

In recent years, there has been a growing trend toward designing receivers with low complexity, utilizing low-resolution ADCs to meet demands for wide bandwidth and reduced cost/power consumption [5, 6]. This approach enables receivers to operate at higher sampling rates with significantly lower implementation overhead compared to conventional high-resolution ADCs [3]–[6]. However, coarse quantization of received signals leads to substantial loss of amplitude and phase information, thereby complicating signal processing and parameter estimation tasks [3], [7].

In [8], a DoA estimation method was proposed DoA estimation for 1-bit ADC systems with deterministic signals, based on sparse matrix recovery. Similarly, for 1-bit ADCs, [9] introduced a lower bound for DoA estimation. Studies [10, 11] evaluated DoA estimation methods for systems with low-resolution and mixed-resolution ADCs. Additionally, machine learning-based DoA estimation techniques have been proposed in [12].

Motivated by these challenges, this paper evaluates common DoA estimation algorithms applicable to low-resolution ADC systems. Furthermore, the Cramér–Rao Lower Bound (CRLB) is derived to assess the fundamental performance limits of these techniques.

The notations used in this paper are as follows: Lowercase and uppercase bold letters denote vectors and matrices, respectively. $\mathbb{C}^{N\times M}$ denotes a complex matrix of size $N \times M$ and $\mathbf{I}_M$ represents an $M \times M$ identity matrix. $|\mathbf{X}|$, $\mathbf{X}^{\mathrm{H}}$, and $\mathrm{tr}(\mathbf{X})$ represent the absolute value, Hermitian transpose, and trace of matrix $\mathbf{X}$, respectively. $\mathrm{E}[\cdot]$ and $\|\cdot\|$ denote expectation and Euclidean norm. A complex random vector or matrix $\mathbf{z}$ with mean μ and variance σ^2 is denoted as $\boldsymbol{z} \sim \mathcal{CN}(\mu, \sigma^2)$. diag() extracts the diagonal of a matrix into a vector or converts a vector into a diagonal matrix.

2. System model

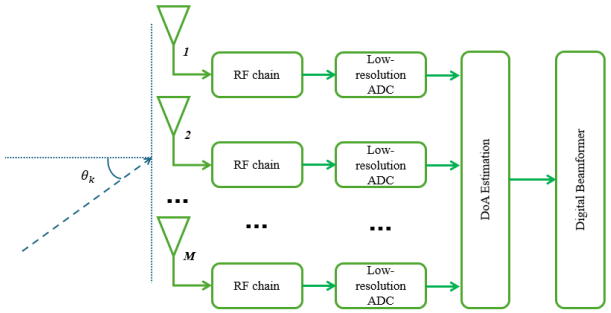

Figure 1. *System model*

Consider the system illustrated in Figure 1, which consists of a uniformly spaced linear array (ULA) with M elements, impinged by K $(K < M)$ independent narrowband sources sharing the same carrier frequency f_c. Let d denote the inter-element spacing, λ the wavelength, θ_k the angle of arrival from the k-th source, and the steering matrix

$\mathbf{A} = [\mathbf{a}(\theta_1), \mathbf{a}(\theta_2), \dots, \mathbf{a}(\theta_K)]^{\boldsymbol{T}} \in \mathbb{C}^{M\times K}$, where

$$\mathbf{a}(\theta_k) = \left[0, e^{j\frac{2\pi d sin\theta_k}{\lambda}}, \dots, e^{j\frac{2\pi(M-1)dsin\theta_k}{\lambda}}\right]^T. \quad (1)$$

Let $s_k(n)$ be the signal from the k-th source at time n, assumed to be independent and Gaussian-distributed with zero mean and variance σ_s^2. The received signal can be modeled as:

$$\mathbf{y}(n) = \sum_{k=1}^{K} \mathbf{a}(\theta_k)s_k(n) + \mathbf{v}(n), \quad (2)$$

where $\mathbf{v}(n)$ is additive white Gaussian noise (AWGN) with zero mean and variance σ_v^2.

Assuming each antenna element is equipped with a low-resolution ADC, the analog received signal is quantized by separately comparing its real and imaginary components with predefined thresholds. For the special case of a 1-bit ADC, each component is quantized to the sign of the input, resulting in a binary representation. The quantized output at the mmm-th antenna is expressed as:

$$\begin{aligned}\mathbf{y}_q(n) &= \alpha\mathbf{y}(n) + \mathbf{v}_q(n)\\ &= \alpha\sum_{k=1}^{K}\mathbf{a}(\theta_k)s_k(n) + \alpha\mathbf{v}(n) + \mathbf{v}_q(n),\end{aligned} \quad (3)$$

Where $\alpha = 1 - \beta$ is the attenuation factor, $\beta = \frac{\mathbb{E}\left[\left|\left|\mathbf{y}-\mathbf{y}_q\right|\right|^2\right]}{\mathbb{E}\left[\left|\left|\mathbf{y}\right|\right|^2\right]}$ represents the ratio between quantization error variance and input variance (ADC distortion), and $\mathbf{v}_q$ is quantization noise assumed to be Gaussian $(\mathcal{CN}(0, \mathbf{R}_{v_q}))$. The values of β can be determined based on the quantization bits as in [13]. For fixed channel identification, let $\mathbf{R}_k$ be the covariance matrix of the k-th source signal, from (3), the covariance matrix of the post-ADC signal can be calculated as:

$$\mathbf{R}_{qq} = \alpha^2\mathbf{R}_{yy} + \mathbf{R}_{v_q}\mathbf{I}_M, \quad (4)$$

where

$$\mathbf{R}_{yy} = \text{diag}(\sum_{k=1}^{K}(\sigma_s^2\mathbf{a}(\theta_k)\,\mathbf{a}^H(\theta_k) + \sigma_v^2)\mathbf{I}_M), \quad (5)$$

and $\mathbf{R}_{v_q} = \beta\text{diag}(\mathbf{R}_{yy})$. (6)

3. Common DoA estimation algorithms

In this section, we introduce several popular DoA estimation algorithms, which will be evaluated in subsequent sections.

From the post-ADC received signal ADC $\mathbf{y}_{qq}(n)$, the estimated covariance matrix is computed as:

$$\widehat{\mathbf{R}}_{qq} = \frac{1}{N}\sum_{n=1}^{N}\mathbf{y}_q(n)\mathbf{y}_q^H(n). \quad (7)$$

3.1. Bartlett algorithm

The Bartlett algorithm [14] is a simple method based on the beamforming spectrum, which calculates the output power of the beamformer for each possible direction to identify the signal direction.

From the estimated ADC covariance matrix, the Bartlett spectrum for each angle is determined by:

$$\boldsymbol{P}_{Bartlett}(\theta) = \mathbf{a}^H(\theta)\,\widehat{\mathbf{R}}_{qq}\,\mathbf{a}(\theta). \quad (8)$$

From (8), the peaks of $P_{Bartlett}(\theta)$ indicate the angles of arrival θ_k corresponding to the incoming signal directions.

The Bartlett algorithm is characterized by low computational complexity and ease of implementation, making it attractive for practical applications. For Gaussian-distributed signals, Bartlett can provide accurate and stable direction-of-arrival (DoA) estimates, particularly when the number of snapshots is sufficiently large.

Nevertheless, its performance degrades in the presence of noise, often leading to biased or inconsistent estimates. In scenarios involving non-Gaussian data, limited sample sizes, or nonlinear signal models, the Bartlett method becomes less effective and may fail to capture the underlying signal structure reliably.

3.2. ESPRIT algorithm

The ESPRIT (Estimation of Signal Parameters via Rotational Invariance Techniques) algorithm exploits the signal subspace structure to estimate the Direction of Arrival (DoA) without spectrum scanning [15]. This method relies on the rotational invariance property of the array to achieve this.

From the covariance matrix, eigenvalue decomposition is performed to identify the signal subspace $\mathbf{E}_s$, which corresponds to the K largest eigenvalues.

$$\widehat{\mathbf{R}}_{qq} = \mathbf{E}_s\boldsymbol{\Lambda}_s\mathbf{E}_s^H + \mathbf{E}_n\boldsymbol{\Lambda}_n\mathbf{E}_n^H, \quad (9)$$

where $\mathbf{E}_s \in \mathbb{C}^{M\times K}$ is the signal subspace. ESPRIT divides $\mathbf{E}_s$ into two subarrays with rotational invariance structure $\mathbf{E}_{s1}$ and $\mathbf{E}_{s2}$. For a ULA, the two subarrays can be the first $M-1$ and last $M-1$ elements of $\mathbf{E}_s$.

The matrix $\boldsymbol{\Psi}$ is determined such that $\mathbf{E}_{s1}\boldsymbol{\Psi} = \mathbf{E}_{s2}$, i.e.,

$$\boldsymbol{\Psi} = \mathbf{E}_{s1}^{+}\mathbf{E}_{s2}. \quad (10)$$

where $\mathbf{E}_{s1}^{+}$ is the pseudoinverse of $\mathbf{E}_{s1}$. Further eigenvalue decomposition of $\boldsymbol{\Psi}$ yields ϕ_k, the eigenvalues of $\boldsymbol{\Psi}$, from which θ_k is computed as::

$$\theta_k = \arcsin\left(\frac{\arg(\phi_k)\lambda}{2\pi d}\right). \quad (11)$$

The ESPRIT algorithm offers high estimation accuracy and is particularly robust under noisy conditions. It is

capable of resolving closely spaced sources and avoids exhaustive parameter-space searches, thereby reducing computational complexity. In addition, ESPRIT demonstrates strong performance when applied to complex or correlated signal models.

Despite these advantages, ESPRIT generally requires a relatively large number of sensors or a sufficiently large array aperture to achieve desirable accuracy, which may limit its practicality in constrained systems. Furthermore, when impinging signals are correlated or not statistically independent, the method can suffer from performance degradation and may yield biased estimates.

3.3. SPICE algorithm

The SPICE (Sparse Iterative Covariance-based Estimation) algorithm is an advanced method for DoA estimation in radar, sonar, or wireless communication systems [16].

SPICE is a convex optimization-based approach that reconstructs the covariance matrix from a sparse signal model. This algorithm does not require prior knowledge of the number of sources and performs well even at low signal-to-noise ratios (SNR).

Assuming the transmitted signals only exist at certain angles (sparsity), the covariance matrix can be expressed as:

$$\mathbf{R} = \mathbf{A}\mathbf{P}\mathbf{A}^H + \sigma^2\mathbf{I}, \tag{12}$$

Where, $\mathbf{A}$ is the steering matrix, $\mathbf{P}$ is a diagonal matrix containing the source powers, and σ^2 is the noise power.

SPICE solves the following convex optimization problem to find the spectrum $\mathbf{P}$:

$$\min \| \boldsymbol{R} - (\boldsymbol{APA^H} + \sigma^2\boldsymbol{I}) \|_F . \tag{13}$$

This problem is solved using iterative methods. The higher the number of iterations, the greater the accuracy of SPICE, albeit with increased algorithmic complexity. Once $\mathbf{P}$ is obtained, the angles corresponding to the largest p_k values are selected as the DoA estimates.

The SPICE algorithm is capable of delivering accurate DoA estimates, particularly in scenarios involving multiple impinging sources. It exhibits robustness against noise, thereby maintaining estimation consistency, and is relatively straightforward to implement without requiring stringent assumptions about the signal or noise environment.

On the other hand, SPICE typically demands a large number of sensors or snapshots to achieve optimal accuracy, which may limit its feasibility in resource-constrained systems. Moreover, the method can experience difficulties when faced with incomplete data or heterogeneous covariance structures. Another drawback lies in its iterative optimization framework: parameter tuning is nontrivial and often requires substantial domain expertise to ensure stable convergence and reliable performance.

3.4. MUSIC algorithm

The MUSIC (MUltiple SIgnal Classification) algorithm is a subspace-based method that utilizes the noise subspace to achieve high-resolution DoA estimation [17].

Similar to ESPRIT, MUSIC performs eigenvalue decomposition of $\widehat{\mathbf{R}}_{qq}$ to identify the noise subspace $\mathbf{E}_n$, corresponding to the $M-K$ smallest eigenvalues. Since $\mathbf{a}(\theta k)$ is orthogonal to the noise subspace: $\mathbf{a}^H(\theta_k)\mathbf{E}_n = \mathbf{0}$, from (7), the MUSIC spectrum is defined as:

$$\boldsymbol{P}_{MUSIC}(\theta) = \frac{1}{\mathbf{a}^H(\theta)\mathbf{E}_n\mathbf{E}_n^H\mathbf{a}(\theta)}. \tag{14}$$

In (14), $\mathbf{E}_n\mathbf{E}_n^H$ is the projection matrix onto the noise subspace. When $\theta = \theta_k$, the denominator approaches zero, resulting in prominent peaks in $P_{MUSIC}(\theta)$. The noise subspace $\mathbf{E}_n$ contains information about directions with no signal. When θ coincides with the true direction θ_k, $\mathbf{a}(\theta)$ is orthogonal to $\mathbf{E}_n$, leading to a peak in the MUSIC spectrum.

To estimate θ_k, scan θ over the range $[-90^0, 90^0]$ and select the K largest peaks in $P_{\mathrm{MUSIC}}(\theta)$, corresponding to the angles of arrival.

MUSIC is a powerful and accurate method for DoA estimation. It can resolve signals arriving from closely spaced directions, which is crucial in practical applications. Additionally, MUSIC performs effectively with a relatively small number of sensors and is applicable to various signal types and models, including non-homogeneous signals.

However, MUSIC may require complex computations and long execution times, especially for large-scale problems. Its application depends on the specific characteristics of the problem and the data.

4. CRLB formula

In this section, we derive the Cramér-Rao Lower Bound (CRLB) for DoA estimation in systems with low-resolution ADCs. To obtain the CRLB, the Fisher Information Matrix (FIM) must first be determined. According to [9, 18], the FIM is computed based on the log-likelihood function of the observed data $\boldsymbol{y}_q(n)$.

Since $\mathbf{y}(n) \sim \mathcal{CN}(0, \mathbf{R}_{yy})$ (as $s(n)$ and $\mathbf{v}(n)$ are Gaussian), and $\mathbf{v}_q(n)$ is also assumed to be Gaussian, $\mathbf{y}_q(n)$ is Gaussian. The probability density function of $\mathbf{y}_q(n)$ is given by:

$$p(\mathbf{y}_q(n)|\theta) = \frac{1}{\pi^M \det(\mathbf{R}_{qq})}\exp\left(-\mathbf{y}_{q(n)}^H\mathbf{R}_{qq}^{-1}\mathbf{y}_q(n)\right). \tag{15}$$

For N independent samples, the log-likelihood function $\left(\mathcal{L} = \log p(\boldsymbol{y}_q(n)|\theta)\right)$ is defined as:

$$\mathcal{L} = -M\log\pi - \log\det(\boldsymbol{R}_{qq}) - \boldsymbol{y}_q(n)^H\boldsymbol{R}_{qq}^{-1}\boldsymbol{y_q}(n). \tag{16}$$

The FIM is defined by [17]:

$$\mathbf{F}(\theta)_{ij} = E\left[\frac{\partial\mathcal{L}}{\partial\theta_i}\frac{\partial\mathcal{L}}{\partial\theta_j}\right] \tag{17}$$

We have:

$$\frac{\partial\mathcal{L}}{\partial\theta_i} = -\frac{\partial\log\det(\mathbf{R}_{qq})}{\partial\theta_i} - \frac{\partial}{\partial\theta_i}\left(\mathbf{y}_q(n)^H\mathbf{R}_{qq}^{-1}\mathbf{y}_q(n)\right). \tag{18}$$

Where $\frac{\partial\log\det(\boldsymbol{R}_{qq})}{\partial\theta_i} = \mathrm{tr}\left(\mathbf{R}_{qq}^{-1}\frac{\partial\boldsymbol{R}_{qq}}{\partial\theta_i}\right)$

and $\frac{\partial}{\partial\theta_i}\left(\mathbf{y}_q(n)^H\mathbf{R}_{qq}^{-1}\mathbf{y}_q(n)\right) = -\mathbf{y}_q(n)^H\mathbf{R}_{qq}^{-1}\frac{\partial\boldsymbol{R}_{qq}}{\partial\theta_i}\mathbf{R}_{qq}^{-1}\mathbf{y}_q(n)$.

Thus,

$$\frac{\partial\mathcal{L}}{\partial\theta_i} = -\mathrm{tr}\left(\mathbf{R}_{qq}^{-1}\frac{\partial\mathbf{R}_{qq}}{\partial\theta_i}\right) + \mathbf{y}_q(n)^H\mathbf{R}_{qq}^{-1}\frac{\partial\boldsymbol{R}_{qq}}{\partial\theta_i}\mathbf{R}_{qq}^{-1}\mathbf{y}_q(n). \tag{19}$$

Using the Slepian-Bangs formula for Gaussian signals, the FIM is given by:

$$\mathbf{F}(\theta)_{ij} = N\,\Re\mathrm{e}\left\{\mathrm{tr}\left(\mathbf{R}_{qq}\frac{\partial \mathbf{R}_{qq}}{\partial \theta_i}\mathbf{R}_{qq}^{-1}\frac{\partial \mathbf{R}_{qq}}{\partial \theta_j}\right)\right\}. \quad (20)$$

From equation (4), we have:

$$\frac{\partial \mathbf{R}_{qq}}{\partial \theta_i} = \alpha^2\frac{\partial \mathbf{R}_{yy}}{\partial \theta_i} + \beta\frac{\partial\,\mathrm{diag}(\mathbf{R}_{yy})}{\partial \theta_i}. \quad (21)$$

Where:

$$\frac{\partial \boldsymbol{R}_{yy}}{\partial \theta_i} = \sigma_i^2\left(\frac{\partial \boldsymbol{a}(\theta_i)}{\partial \theta_i}\boldsymbol{a}(\theta_i)^H + \boldsymbol{a}(\theta_i)\frac{\partial \boldsymbol{a}^H(\theta_i)}{\partial \theta_i}\right)$$

and

$$\frac{\partial \boldsymbol{a}(\theta_i)}{\partial \theta_i} = \frac{j2\pi d}{\lambda}\cos\theta_i\left[0, 1e^{\frac{j2\pi d}{\lambda}\sin\theta_i}, \ldots, (M-1)\,e^{\frac{j2\pi d}{\lambda}(\mathrm{M}-1)\sin\theta_i}\right]^T \odot \boldsymbol{a}(\theta_i).$$

Once the FIM is determined, the CRLB for θ_k is the minimum achievable variance of any unbiased estimator of θ_k:

$$CRLB(\theta) = [\mathbf{F}^{-1}(\theta)]_{kk}. \quad (22)$$

Here, $\mathbf{F}(\theta)$ is a $K \times K$ matrix with each element computed as in (20).

5. Results and discussion

In this section, we conduct various simulation scenarios to evaluate DoA estimation techniques using low-resolution ADC data. The simulations are implemented in Python, utilizing the numpy and scipy libraries for computation, and matplotlib for visualization.

The simulation parameters are presented in Table 1. In all experiments, 1000 random data samples (channel realizations) are generated.

Table 1. *Simulation setup parameters.*

Parameter	Value
The number of antenna M	8, 64, 128
The number of snapshot N	32
Distance between antennas d	$\lambda/2$
True DoA θ	15, 30, 45
Signal to noise ratio SNR	-10 – 20dB

Figure 3 compares DoA estimation techniques for angle $\theta = 45^0$ in systems with 4-bit ADCs and $M = 8$, 64 at SNR = 20dB. The results indicate that ESPRIT fails to provide reliable DoA estimates in systems employing low-resolution ADCs. Heavy quantization causes severe distortion of both phase and amplitude information, which undermines the algorithm's assumptions. Since ESPRIT depends on accurate characterization of the signal subspace and the rotational invariance property between subarrays, coarse quantization prevents the estimated covariance matrices from preserving the true spatial relationships among antenna elements. Moreover, the covariance matrix $\mathbf{R}_{qq}$ tends to be ill-conditioned under coarse quantization, which severely affects eigenvalue and eigenvector analysis, thereby reducing ESPRIT's accuracy. Bartlett, SPICE, and MUSIC exhibit spectrum energy concentrated at the angles of arrival. As the number of antennas increases, these methods yield increasingly accurate estimates.

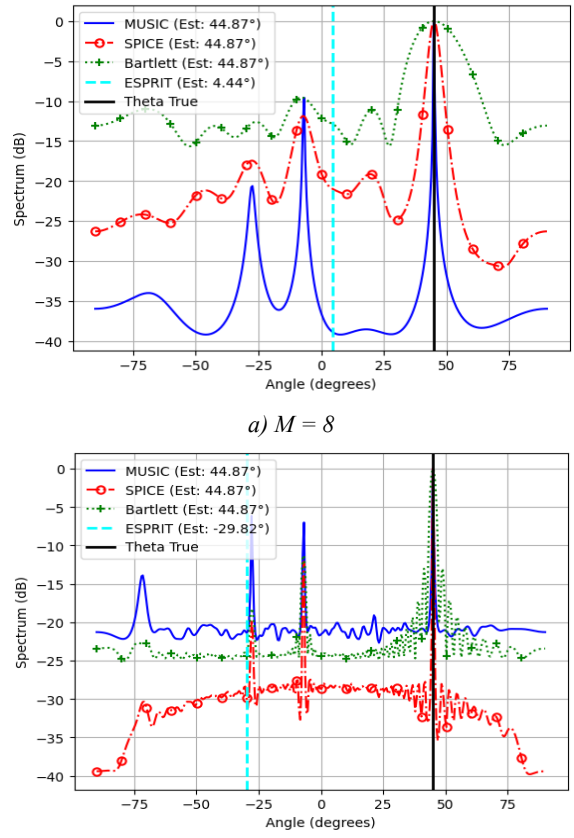

a) M = 8

b) M=64

Figure 3. *DoA estimation techniques with arrival angle $\theta = 45^0$ in 4-bit ADC system with M =8.*

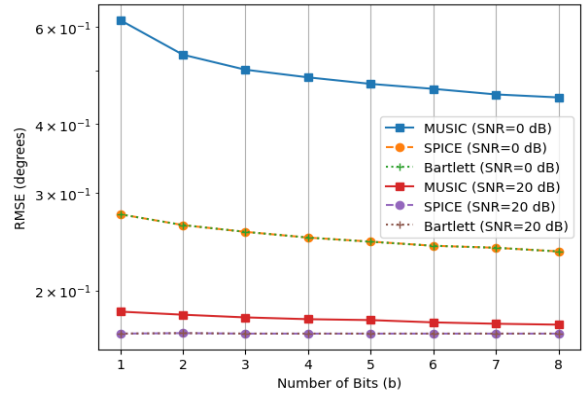

Figure 4. *RMSE is a function of the number of quantized bits with SNR = {0, 20}dB, $\theta = 30^0$*

Figures 4 and 5 compare DoA estimation algorithms with respect to quantization bits and SNR for angle $\theta = 30^0$in ADC systems. In both figures, SPICE and Bartlett provide more accurate estimates than MUSIC, as they are less sensitive to loss of phase/amplitude information. Figure 5 also presents the CRLB together with the evaluated estimation methods. As the SNR increases, the RMSE decreases, reflecting improved estimation accuracy. Under coarse quantization, MUSIC exhibits inferior performance compared to Bartlett and SPICE. Nevertheless, at high SNR and in scenarios where quantization is less severe, MUSIC can be advantageous due to its superior angular resolution, particularly when combined with algorithmic enhancements. Furthermore,

the persistent performance gap between DoA estimation methods in low-resolution ADC systems and the CRLB highlights opportunities for developing improved techniques to narrow this gap, representing an open avenue for future research.

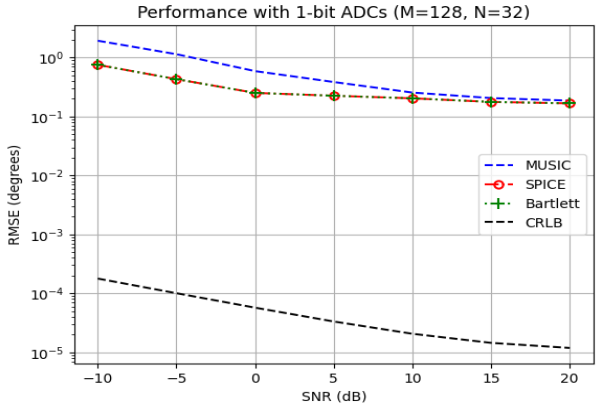

Figure 5. *Evaluation of DoA Estimation Techniques in SNR with b= 3 bit, $\theta = 30^0$*

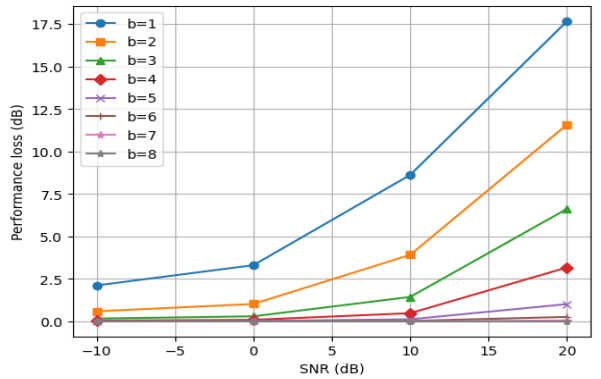

Figure 6. *Performance loss as a function of SNR*

Figure 6 depicts the performance loss $\eta_b = 10\log_{10}\frac{CRLB_b}{CRLB_\infty}(dB)$ theo SNR versus SNR for different quantization bit values b in the ADC system. From the figure, it can be seen that the performance loss factor η_b increases with SNR for a fixed number of quantization bits. For 1-bit ADCs, the performance loss is more than 2 dB compared to other cases across all SNR values. In the low-SNR regime, 2-bit ADCs can be used, while in the high-SNR regime, ADCs with higher quantization bits (4 or 5 bits) are recommended. Thus, for most applications with moderate SNR, 2- or 3-bit ADCs are optimal.

6. Conclusion

In this paper, we review common DoA estimation algorithms and derive the Cramér–Rao lower bound (CRLB) for systems employing low-resolution ADCs. Simulation results demonstrate that MUSIC, SPICE, and Bartlett methods exhibit degraded accuracy under coarse quantization, indicating room for further enhancement. Moreover, the findings suggest that employing ADCs with 2–3 quantization bits offers an effective balance between estimation performance and hardware efficiency.

Acknowledgment: This research is funded by the Ministry of Education and Training under the project code B2024.DNA.13.

REFERENCES

[1] H. L. Van Trees, *Optimum Array Processing (Detection, Estimation, and Modulation Theory, Part IV)*. New York, NY, USA: Wiley, 2002.

[2] S. S. Haykin, J. Litva, and T. J. Shepherd, Eds., *Radar Array Processing. Berlin*, Germany: Springer-Verlag, 1993.

[3] S. Sedighi, B. S. Mysore R, M. Soltanalian, and B. Ottersten, "On the performance of one-bit DoA estimation via sparse linear arrays", *IEEE Trans. Signal Process.*, vol. 69, pp. 6165–6182, 2021, doi: 10.1109/TSP.2021.3122290.

[4] D. K. W. Ho and B. D. Rao, "Antithetic dithered 1-bit massive MIMO architecture: Efficient channel estimation via parameter expansion and PML", *IEEE Trans. Signal Process*., vol. 67, no. 9, pp. 2291–2303, May 2019.

[5] O. Orhan, E. Erkip, and S. Rangan, "Low power analog-to-digital conversion in millimeter wave systems: Impact of resolution and bandwidth on performance", *arXiv preprint* arXiv:1502.01980, 2015.

[6] J. Mo and R. W. Heath Jr., "Capacity analysis of one-bit quantized MIMO systems with transmitter channel state information", *IEEE Trans. Signal Process.*, vol. 63, no. 20, pp. 5498–5512, Oct. 2015.

[7] F. Yeganegi, A. Eamaz, and M. Soltanalian, "Low-rank matrix sensing with dithered one-bit quantization", in *Proc. IEEE Int. Symp. Inf. Theory (ISIT)*, 2024, pp. 527–532.

[8] M. Chen, Q. Li, X. P. Li, L. Huang, and M. Rihan, "One-bit DoA estimation for deterministic signals based on $\ell_{2,1}$-norm minimization", *IEEE Trans. Aerosp. Electron. Syst.*, vol. 60, no. 2, pp. 2438–2444, Apr. 2024, doi: 10.1109/TAES.2023.3348084.

[9] M. Chen, Q. Li, L. Huang, L. Feng, and M. Rihan, "One-bit Cramér–Rao bound of direction of arrival estimation for deterministic signals", *IEEE Trans. Circuits Syst. II, Exp. Briefs*, vol. 71, no. 2, pp. 957–961, Feb. 2024, doi: 10.1109/TCSII.2023.3309788.

[10] B. Shi et al., "Impact of low-resolution ADC on DOA estimation performance for massive MIMO receive array", *IEEE Syst. J.*, vol. 16, no. 2, pp. 2635–2638, Jun. 2022, doi: 10.1109/JSYST.2021.3139449.

[11] B. Shi, Q. Zhang, R. Dong, Q. Jie, S. Yan, F. Shu, and J. Wang, "DOA estimation for hybrid massive MIMO systems using mixed-ADCs: Performance loss and energy efficiency", *IEEE Open J. Commun. Soc.*, vol. 4, pp. 1383–1395, 2023.

[12] F. Yeganegi, A. Eamaz, T. Esmaeilbeig, and M. Soltanalian, "Deep learning-enabled one-bit DoA estimation", in *Proc. IEEE Sensor Array Multichannel Signal Process. Workshop (SAM)*, Corvallis, OR, USA, 2024, pp. 1–5, doi: 10.1109/SAM60225.2024.10636650.

[13] J. Max, "Quantizing for minimum distortion", *IRE Trans. Inf. Theory*, vol. 6, no. 1, pp. 7–12, Mar. 1960.

[14] M. Bartlett, "Smoothing periodograms from time-series with continuous spectra", *Nature*, vol. 161, pp. 686–687, 1948, doi: 10.1038/161686a0.

[15] F. Gao and A. B. Gershman, "A generalized ESPRIT approach to direction-of-arrival estimation", *IEEE Signal Process. Lett.*, vol. 12, no. 3, pp. 254–257, Mar. 2005.

[16] P. Stoica, P. Babu, and J. Li, "SPICE: A sparse covariance-based estimation method for array processing", *IEEE Trans. Signal Process.*, vol. 59, no. 2, pp. 629–638, Feb. 2011.

[17] P. Vallet, X. Mestre, and P. Loubaton, "Performance analysis of an improved MUSIC DoA estimator", *IEEE Trans. Signal Process.*, vol. 63, no. 23, pp. 6407–6422, Dec. 2015.

[18] S. M. Kay, *Fundamentals of Statistical Signal Processing: Estimation Theory*. Englewood Cliffs, NJ, USA: Prentice-Hall, 1993.